The following appendix accompanies the article

FEATURE ARTICLE

Oceanic circumpolar habitats of Antarctic krill

A. Atkinson[1,*], V. Siegel[2], E. A. Pakhomov[3,4], P. Rothery[5], V. Loeb[6], R. M. Ross[7], L. B. Quetin[7], K. Schmidt[1], P. Fretwell[1], E. J. Murphy[1], G. A. Tarling[1], A. H. Fleming[1]

[1]British Antarctic Survey, Natural Environment Research Council, High Cross, Madingley Road, Cambridge CB3 0ET, UK
[2]Sea Fisheries Institute, Palmaille 9, 22767 Hamburg, Germany
[3]Department of Earth and Ocean Sciences, University of British Columbia, 6339 Stores Road, Vancouver, BC V6T 1Z4, Canada
[4]Department of Zoology, Faculty of Science and Technology, University of Fort Hare, Private Bag X1314, Alice 5700, South Africa
[5]Centre for Ecology and Hydrology, CEH Monks Wood, Abbots Ripton, Huntingdon PE28 2LS, UK
[6]Moss Landing Marine Laboratories, 8272 Moss Landing Road, Moss Landing, California 95039, USA
[7]Marine Science Institute, University of California at Santa Barbara, Santa Barbara, California 93106-6150, USA

*Email: aat@bas.ac.uk

Marine Ecology Progress Series 362:1–23 (2008)

Appendix 1. Methodology

'KRILLBASE': an historical database of postlarval krill density

The full database, with 9922 individual net hauls, is a multi-national composite (1926 to 1939, 1976 to 2004). It expands on a previous version (Atkinson et al. 2004) with >2000 more records and extended seasonal coverage of October–April. It also combines, for the first time, datasets from 'Discovery', AMLR, Palmer LTER, ANARE, JARE, BIOMASS, CCAMLR and other surveys (Table A1). Most (76%) of sampling was in December–February. A critical point is that all KRILLBASE records are from pre-fixed stations (i.e. not targeted) with scientific nets rather than commercial trawls whose mouth areas are poorly known.

From the full database in Table A1, we further excluded from statistical analysis all data north of the Antarctic Polar Front (APF), in order to include only the normal distributional range of *Euphausia superba* (Marr 1962). Also excluded were all horizontal hauls or those whose top sampling depth was >20 m or bottom depth was <50 m. Most hauls were to >100 m and the top depth was the surface at 96% of stations.

Data for KRILLBASE were obtained from a variety of sources (Table A1), but most were from the authors' institutes. However, collaborators from other nations working around Antarctica kindly sent further data to give KRILLBASE a more fully international and circumpolar scope. A few records were taken directly from publications. The historical data from the 'Discovery' Investigations (1926–1951) were extracted from records archived in the library of the National Oceanography Centre Southampton (NOCS, UK). These data were drawn from 2 sources: the net sampling logs and the original master tables used to construct the figures of Marr (1962). These were cross-checked with an electronic krill database of 'Discovery' data held at the British Antarctic Survey (BAS). Krill densities (ind. m^{-2}) were calculated from published dimensions of the nets and sampling information provided by the 'Discovery' Report station lists.

Even with such a high number of stations, spatial coverage was highly uneven (Fig. A1). The Atlantic sector was best covered, with good coverage also along the Greenwich Meridian and Prydz Bay area.

Standardisation of krill densities within KRILLBASE

Although only non-targeted scientific net haul surveys were used for this database, the data were derived from a composite of surveys which differ in sampling depth, gear used, proportion of day vs. night hauls, and time of year of sampling. All of these could potentially alias the horizontal distribution patterns of interest. Each of the above problems were removed as far as is possible by analysis and the application of appropriate conversion factors. This approach is analogous to those by 'Discovery' scientists (Marr 1962, Mackintosh 1973) to produce their maps of krill distribution.

We could not adjust for year of sampling given the paucity of sampling years in some sectors, and the fact that interannual variation might not be in phase throughout Antarctica. We thus converted all observed densities to a standard and defined methodology—a night-time 0 to 200 m haul with an RMT8 net on 1 January. This yields near maximum densities achievable by scientific nets.

When examined simultaneously and across the whole database, these sampling effects can interact among each other and they vary spatially. However, we were able to isolate the effects of sampling depth and time of day in separate analyses of specific data subsets, and then further examine issues of net mouth area and time of year of sampling on data already adjusted for sampling depth and time of day. We tested the robustness of these conversion factors pragmatically by comparing our major results based on corrected and uncorrected densities.

Sampling depth of the net

After the initial screening of the database according to top and bottom sampling depths (see above), mean krill density from net hauls entirely within the top 200 m was 19.1 ind. m^{-2} (median 0.1, 8190 hauls) whereas hauls from deeper yielded 0.532 ind. m^{-2} (median 0, 855 hauls). This supports other analyses (Godlewska 1996, Siegel 2005) that most krill reside within the top 200 m during summer. Our purpose therefore was to apply appropriate multiplication factors to nets sampling to less than 200 m, in order

Table A1. Summary of sampling details for KRILLBASE (9922 hauls). Component datasets are listed in order of size, and divided into blocks according to nation and data source. Publications are listed where these were the major source of the data. GAMLR = German Antarctic Marine Living Resources surveys, BIOMASS = Biological Investigations of Marine Antarctic Systems and Stocks, SIBEX = Second International Biomass Experiment, AMLR = Antarctic Marine Living Resources, LTER = Long-Term Ecological Research, BAS = British Antarctic Survey, ANARE = Australian National Research Expedition, CCAMLR = Convention for the Conservation of Antarctic Marine Living Resources, 'FRUELA' = name of 8th century king, JARE = Japanese Antarctic Research Expedition, BROKE = Baseline Research on Oceanography, Krill and the Environment, RMT = Rectangular Midwater Trawl, IKMT = Isaacs Kidd Midwater Trawl. Note that only subsets of this full database were extracted for our analyses

Dataset, nation	Location	Seasons	No. of hauls	Main net types	Mean sampling depth (m)	Source
GAMLR data, including e.g. SIBEX data from BIOMASS programme (Germany)	Circumpolar	1976, 1978, 1980–1982, 1984–1986, 1988–1990, 1995, 1997, 2001, 2004	2375	RMT8, IKMT	169	Siegel supplied original data
AMLR Program (USA)	Antarctic Peninsula/ Elephant Island	1990–1991, 1993–2003	1960	IKMT	169	Loeb, Hewitt supplied original data
'Discovery' Investigations (UK)	Circumpolar	1926–1939, 1951	1564	N100B (1 m ringnet)	159	(archived data extracted by Atkinson)
Various datasets (Ukraine)	Circumpolar	1982–1990, 1992, 1996, 1997	1491	IKMT, Bongo, modified Juday net and Melnikov trawl	149	Pakhomov supplied original data
BAS data (UK)	South Georgia, Scotia Sea, Antarctic Peninsula	1980, 1982, 1985, 1996–1999, 2001–2003	740	RMT8, Bongo	346	From BAS and SIBEX data holdings
LTER grid data (USA)	Western Antarctic Peninsula	1993–2003	635	2 m square sided fixed frame net	122	Ross, Quetin supplied original data
Various datasets (South Africa)	Atlantic/Indian sectors	1981, 1993, 1995, 1997, 1998, 2001, 2003	318	Bongo net, RMT8	268	Pakhomov supplied original data
1990s surveys (Australia)	Prydz Bay, and east in Indian sector (BROKE)	1991, 1993, 1996	213	RMT8	199	Hosie supplied original data
1980s surveys (Australia)	Indian sector	1981, 1983, 1985, 1987	167	RMT8, 0.5 m and 1 m diameter nets	335	ANARE Research Notes
Published data (Poland)	Antarctic Peninsula	1981, 1984	160	Bongo and Nansen nets	197	Jazdewski et al. (1982), Witek et al. (1985)
CCAMLR Synoptic survey (multinational)	SW Atlantic sector	2000	119	RMT8	201	CCAMLR supplied original data
FRUELA data, (Spain)	Antarctic Peninsula	1996	99	Modified WP2 net	200	Anadon supplied original data
JARE data (Japan)	Indian sector	1988–1990, 1992–1996	68	ORI, NORPAC	165	Chiba supplied original data
SIBEX data (Japan)	South of Australia	1984	13	Large IKMT	723	Terazaki & Wada (1986)

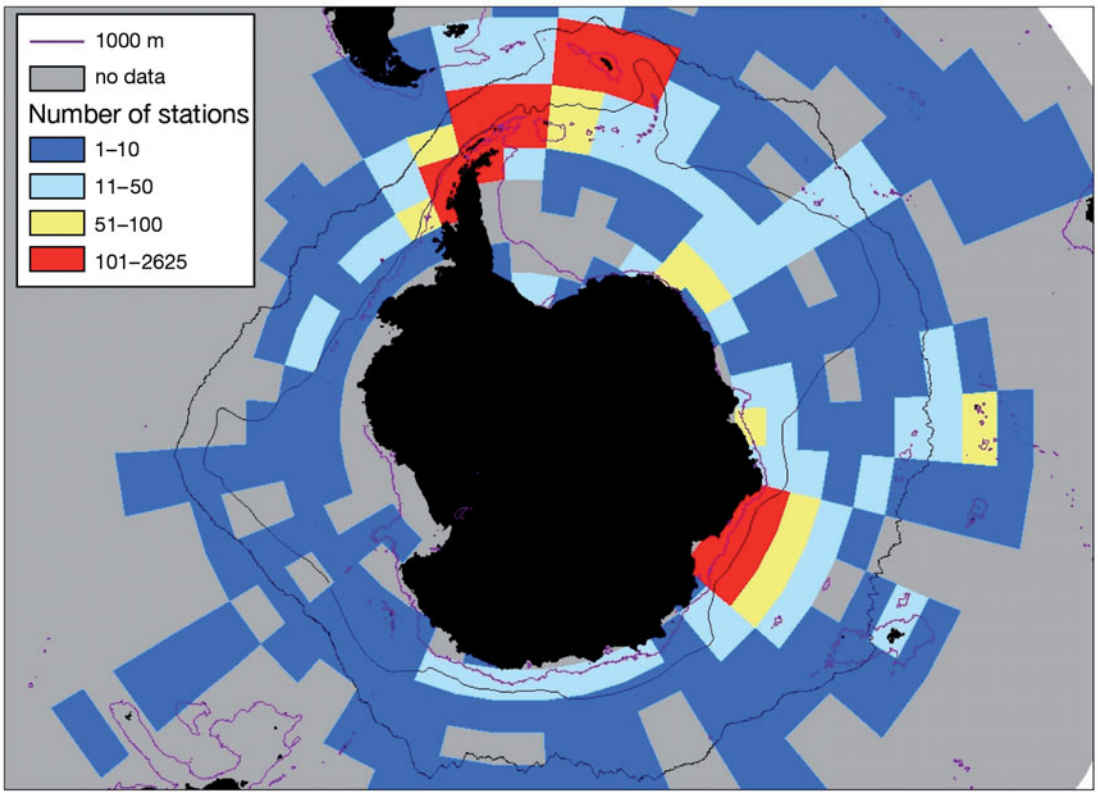

Fig. A1. Distribution of sampling coverage, based on all stations in the final reduced database. Fronts (black lines), from north to south are Antarctic Polar Front (APF) and Southern Boundary of the Antarctic Circumpolar Current (SB-ACC). Grey area signifies no data

to make catches equivalent to those from the entire top 200 m layer.

Information on the vertical distribution of krill in our database is most reliably obtained by analysis of the vertically-stratified series of net hauls. From these we excluded series in which krill density was < 1 ind. m^{-2} because of potential artefacts due to contamination and net leakage at low krill densities. We further refined the subset to 85 stratified net series (262 hauls) where top depth was <5 m and bottom depth was 195 to 250 m. There was a hyperbolic relationship between total density, f and bottom depth, x (m). Constraining this for $f = 1$ when $x = 200$ m, then

$$f = Ax/[1 + x(A - 0.005)] \quad (A1)$$

where A is a constant. We fitted a LOWESS line to the relationship and chose A to match the value of the LOWESS line at $x = 50$, i.e. $f = 0.88$.

This gives

$$f = 0.11x/(1 + 0.105x) \quad (A2)$$

Thus, based on the values of f, all catches from nets fishing to <200 m were corrected to those of a 0 to 200 m equivalent haul.

Time of day

Almost all krill catch records had information either on sampling time or on whether the samples were collected during day or night. To maximise consistency we applied a standard algorithm (http://search.cpan.org/~rkhill/Astro-Sunrise-0.91/Sunrise.pm) to define sunrise and sunset times based on latitude, longitude, and date, and then coded hauls as either day or night based on sampling time. Night was defined as the duration when the sun's altitude is <–0.833 degrees (when its upper limb touches the horizon with atmospheric refraction accounted for).

Adjustments for day/night based on analyses of the entire database are inappropriate, as the proportions of night-time hauls also vary with latitude and time of year, both of which also have direct effects on krill density. Therefore, to minimize this aliasing we analysed two large monitoring surveys from the Antarctic Peninsula (AMLR and Palmer LTER: see Table A1) where nets were towed effectively at random times of day and night in defined geographical areas. Analysis of these combined 2595 hauls gave a ratio of median density at night versus day of 2.255 and a ratio of mean density at night versus day of 2.156. Thus all daytime densities were multiplied by 2.255.

Net mouth area and time of year of sampling

Adjustments for sampling depth and day/night could be performed on large subsets of the data that were not biased by major differences in krill density between sectors. This was not possible when adjusting for mouth area and time of year of sampling due to the heterogeneous coverage of the data. However, to avoid potentially large regional biases in our adjustment model, we restricted the input data to that

south of the APF from 10 to 80° W. This is a sector of relatively uniform and high krill density compared to other sectors, thus minimizing spatial bias while preserving a large sample size (6705 stations).

Krill densities at these stations were bimodally distributed with a high proportion of zeros. (Note that the adjustments above are multiplicative and do not alter the values of zero catches). This bimodality required 2 approaches. Firstly, we used logistic binary regression for the probability, P, of returning a non-zero krill density and secondly, for non-zero densities we used a general linear model.

The logistic regression is of the form:

$$P = \exp(L)/[1 + \exp(L)] \quad \text{(A3)}$$

where

$$L = -0.6478 + 2.335\log_{10}M + 0.0204J - 0.0001086J^2 \quad \text{(A4)}$$

and where P is the probability of returning a non-zero catch, M is the nominal mouth area of the net (m^2) and J is the day of sampling (October 1st = 1).

These non-zero densities $K_{\text{non-zero}}$ were related to M and J as:

$$\text{Log}_{10}(K_{\text{non-zero}}) = 0.474 - 0.1912\log_{10}M + 0.00416J - 0.00002898J^2 \quad \text{(A5)}$$

Combining these 2 components yields the predicted krill density, K_{pred}, for each net haul of the database:

$$K_{\text{pred}} = P\,K_{\text{non-zero}} \quad \text{(A6)}$$

Standardised krill density, K_{stan}, was then calculated for each net haul as:

$$K_{\text{stan}} = K_{\text{obs}}(K_{\text{pred-RMT8}}/K_{\text{pred}}) \quad \text{(A7)}$$

where K_{obs} is the observed density (after adjusting for net depth and day/night) and $K_{\text{pred-RMT8}}$ is the density predicted from our model for the values of our optimum netting combination.

Effects of density standardisation

The form of the adjustment model, illustrated in Fig. A2, is consistent with expectations. Adjustment factors are minimal for samples taken during the months of December and January (Days 61 to 123) when the postlarval population is swelled by the year's new recruits. After this time, mortality (and possibly autumnal vertical migration; Siegel 2005) progressively reduce the population, requiring substantial adjustments to stations sampled in autumn. Likewise, the adjustment factors for net mouth area follow expected relationships. There is comparatively little difference among the catching efficiencies of the large nets, but nets with mouth openings of 1 m^2 and smaller (many of which have bridles, release-gear or towing wires running in front of the net) have rapidly diminishing efficiencies that require compensatory high adjustments. We stress that most net sampling was from large nets in midsummer, resulting in modest adjustment factors. Overall mean densities within the database are 2.47-fold those of unadjusted data. Poor sampling combinations (e.g. daytime hauls with small nets late in the season) were the exception.

Except where stated otherwise, all results presented in the main paper are based on standardised densities, adjusted to a single and efficient net sampling method.

Fig. A3 compares large-scale density distributions based on unadjusted and standardised krill densities. These show the same basic trends despite higher overall densities after standardisation. The variability in sampling density, combined with patchy distribution of krill, leads to a mosaic of high and low density, especially in the more poorly sampled regions outside of the SW Atlantic sector. However, following standardisation this 'patchwork' picture is slightly smoother, particularly in the Indian sector regions closest to the continent. This reflects areas within this sector (notably between the Greenwich meridian and Prydz Bay) where net size was generally smaller than average and/or sampling was often later in the season than average.

Overall, very similar statistical relationships were observed, whether using standardised or unadjusted data. This is illustrated by the consistency in the relationships between krill density and food (Fig. A3). While the factors influencing net-derived krill density estimates are complex and inter related, these factors have never been addressed together. Faced with a wide array of possible ways of standarising data, we chose a simple and pragmatic approach. The fact that it preserves the basic structures evident in the original dataset provides reassurance that further artefacts have not been introduced.

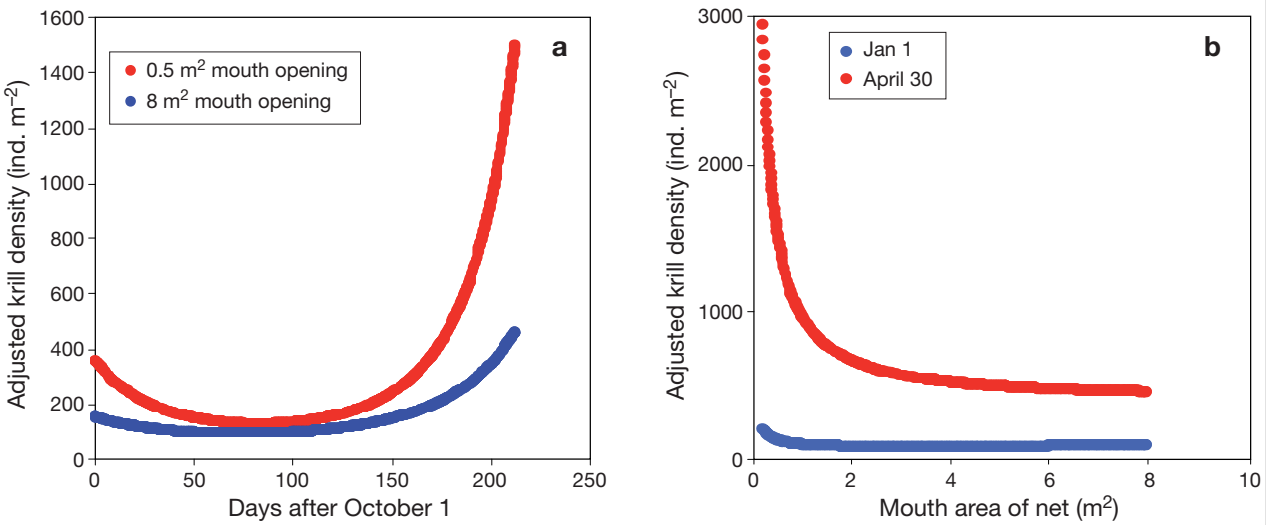

Fig. A2. Behaviour of the density standardisation model, illustrated here to adjust a krill density of 100 ind. m^{-2} (already corrected for sampling depth and time of day) to that of a standardised RMT 8 haul on January 1. (a) Standardised densities for contrasting net sizes for the time-span of the database; (b) standardised densities at 2 times of year across the full range of nominal net mouth areas

Environmental data

Bathymetry data were taken from the GEBCO 2003 Atlas (IOC et al. 2003). Using ArcGIS 9.0 we obtained mean bathymetry values for each net-sampling station based on all pixels within 10 km of it, having excluded any pixels on land. This procedure was used to integrate locally variable bottom topography.

The position of the APF was based on a compilation of satellite data (Moore et al. 1999). The Southern Antarctic Circumpolar Current (AAC) Front (SACCF) and Southern Boundary of the ACC (SB-ACC) were from Orsi et al. (1995), with finer resolution of the SACCF in the Scotia Sea from Thorpe et al. (2002).

The ice edge was defined by the northern extent of the 15% ice concentration in each degree of latitude, based on the DMSP-SSMI passive microwave data by NOAA/NCEP. Average positions for February and September (composite from 1978–2003) were determined having first screened out anomalous records due to icebergs etc.

Chlorophyll *a* (chl *a*) concentrations were obtained from the SeaWiFS standard Level 3 mapped products (NASA) as monthly composite values. Using GIS v.9.0 the 9 × 9 km pixel images were over-layed on a 0.5° latitude by 1° longitude grid to obtain a mean value for each grid cell.

Temperature data were extracted from individual monthly MODIS composites. This particular dataset was used, as it makes no assumptions over water temperatures under sea ice, these values being classed as absent data. We did not want to force our krill growth model (based on the open water season) with data extrapolated from under ice.

Calculation of the proportion of total krill located over the shelf/slope

We define here the 'continental shelf and slope' as that in which water depth is <2000 m. To calculate the proportion of the total krill population within this habitat we plotted their mean densities on a 3° latitude by 9° longitude grid. Within the water area south of the APF we calculated total areas of both deep ocean A_o and shelf/slope water, A_s in each grid cell. All area-based calculations in this paper were based on a Lambert South Polar Azimuthal Equal Area Projection. In any shelf component of the cell krill density, d_s, was calculated from the mean density over the whole cell $D_{overall}$:

$$D_{overall} = [(d_s A_s) + (A_o d_s/1.65)]/(A_s + A_o) \quad \text{(A8)}$$

and the assumption that the ratio between the shelf and oceanic densities was 1.65, based on the overall means for all shelf and oceanic stations. Total abundance of individuals in the shelf portion of the cell was then obtained as a product of d_s and A_s and likewise for those in the oceanic portion. Overall circumpolar abundances in each habitat were then obtained by summation.

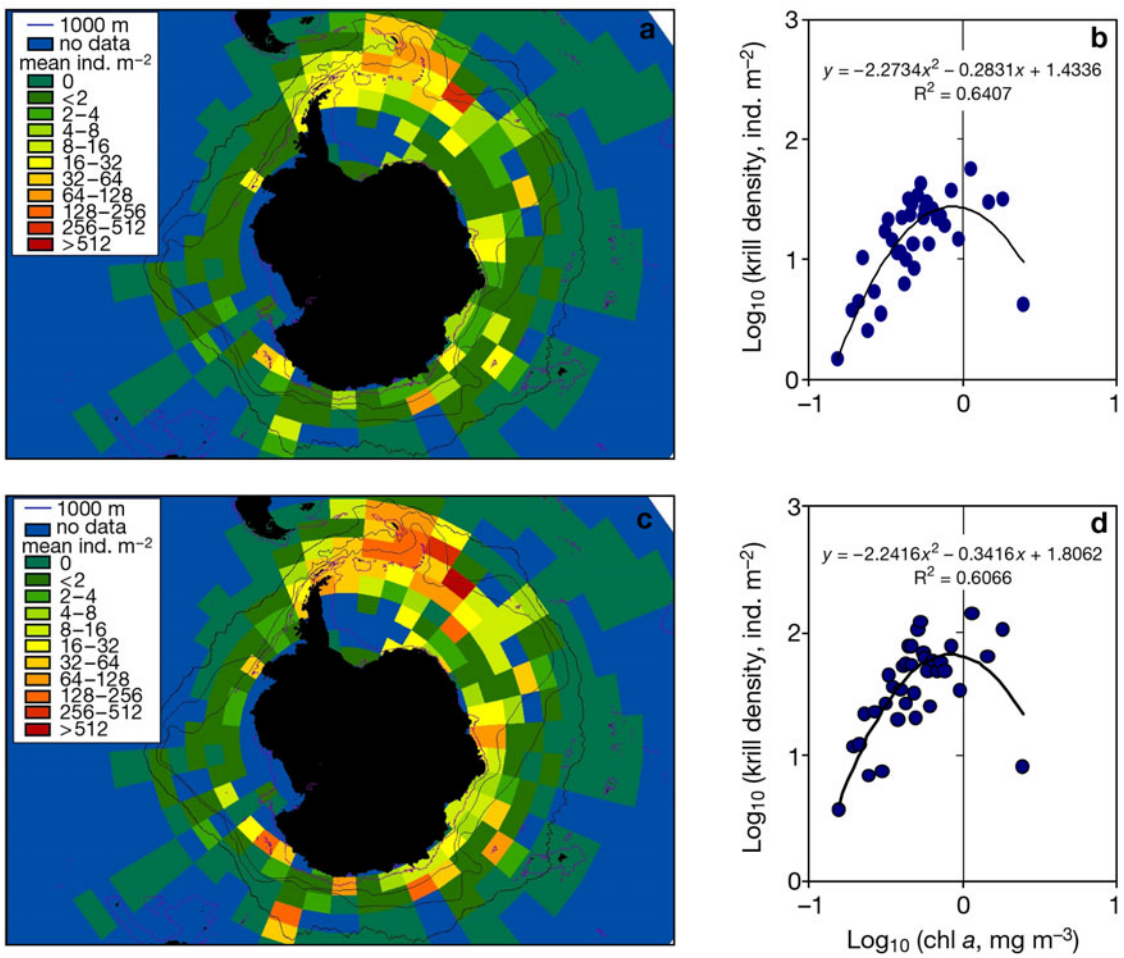

Fig. A3. *Euphausia superba*. Circumpolar distribution of krill densities and the key relationship with chl *a* concentration (see main text 'Bottom-up control factors') before any adjustment factors (a,b) and (c,d) based on standardised densities

Alternative calculations were made by inserting dummy values (i.e of the respective mean overall values shelf and ocean krill densities) into the grid cells with no sampling coverage. This yielded a value of 84% of the total population inhabiting the oceanic habitat, similar to the value of 87% calculated by the first method.

Analysis of krill density in relation to environment

Most krill densities within KRILLBASE were either outside of the SeaWiFS/CZCS (Coastal Zone Colour Scanner) eras or coincided with cloud cover, preventing us from linking them with ambient food concentrations. Here we have adopted a wider scale approach, to develop long-term summer 'climatologies' of food, water temperature, sea ice edge, etc., and to relate the krill distributions to these. Thus, the krill records were projected onto the 0.5° latitude by 1° longitude grid of the mean chl *a* and temperature data to obtain the relevant environmental grid cell mean values and the resultant file was exported for analysis in MINITAB v.14.

We compared krill density data with environmental values in 2 ways, both employing a sample size of 36 for comparable statistics and compatibility with a similar habitat analysis (Nicol et al. 2004). First we used an area-based method, examining the congruence between krill density per sector and its area of elevated chl *a*, shelf/slope and sea ice zone (SIZ). We thus we divided the data south of the APF into 36 sectors of 10° longitude. Within these, we used published data of Nicol et al. (2004) for physical variables. For chl *a* we used areas of >0.5 mg chl *a* m^{-3} from 7 yr December to March 'climatologies'.

The second approach was to rank all the krill density values, with their attached environment climatologies, in ascending order of the environmental predictor (*x*-value) of interest. We then divided this table into 36 groups of equal size (~226 stations) and used the mean *x*- and *y*-values within each group for regression.

Krill growth calculation

To predict daily growth rate (DGR, mm d^{-1}) we used the empirical model of Atkinson et al (2006) based on krill length, *L* (mm), SeaWiFS-derived food, *F* (mg chl *a* m^{-3}) and sea surface temperature, *T* (°C):

$$\mathrm{DGR} = -0.066 + 0.002L - 0.000061L^2 + [0.385C/(0.328 + C)] + 0.0078T - 0.0101T^2 \quad \text{(A9)}$$

This model is designed for use with satellite-derived chl *a* inputs, and is based on a method reflective of *in-situ* growth (Ross et al. 2000, Atkinson et al. 2006, Kawaguchi et al. 2006, Tarling et al. 2006). For each of our 0.5° by 1° grid cells we computed summer growth, starting with a uniform 30 mm long krill in each cell. The model was run for 4 mo from 1 December, using Eq. (A9) for each of the 43 200 grid cells. Thus we based our daily growth calculation on the krill length and the relevant month's satellite-derived temperature and food indices. Absent chl *a* or temperature data within any of the months precluded calculations—extrapolated values were not used. We grew krill for the 4 mo period over each of the 7 summers between 1997–1998 and 2003–2004 and calculated the mean of these. In a separate analysis we grew krill in the same way but starting with a uniform 40 mm population.

We converted DGR from units of krill length *L*, to dry mass, *M* by applying length–mass regressions that were derived from the same krill used to construct the empirical growth model (Atkinson et al. 2006):

$$\log_{10} M = 3.89 \log_{10} L - 4.19 \quad \text{(A10)}$$

In this way we could calculate a Gross Growth Potential (GGP) for each grid cell, *i*:

$$\mathrm{GGP}_i = M_{\mathrm{March\ 31}}/M_{\mathrm{Dec\ 1}} \quad \text{(A11)}$$

where $M_{\mathrm{Dec\ 1}}$ is the predicted mass of the initial 30 mm or 40 mm krill, i.e. 36 mg or 110 mg as predicted from Eq. (10), and $M_{\mathrm{March\ 31}}$ is its final predicted mass after 121 d of growth increments. Note that this calculation is not analagous to a production:biomass (P:B) ratio since it specifically excludes mortality.

As an estimate of total annual growth this value is conservative, being based on only part of the growing season. The model was run from December to March to bracket the January to February period on which the growth model is based, and to maximise the open water period for satellite coverage. However, growth in length occurs as early as September, with a decline after January (Miller & Hampton 1989, Kawaguchi et al. 2006), coincident with spawning (Quetin & Ross 2001) and lipid build-up until April (Hagen et al. 2001). Thus, reductions in somatic growth after January probably reflect diversion of energy towards reproduction and winter survival. These alternative forms of growth are captured in our estimates of GGP, since this is based on mass.

Risk-benefit model of habitat suitability

This model was constructed solely to demonstrate numerically that a trade-off exists between habitats offering high growth reward but high predation risk and those of low reward but low risk. Insufficient data are available on predation rates for circumpolar predictions (e.g. of net growth), so the aim was simply to examine whether predation is indeed a significant factor in this trade-off.

The model was run through January and February, when most data on krill predators are available. The model used water depth as a gradient for this trade-off (see main text for reasons). To calculate growth reward for an individual krill along these gradients in water depth and food (main text Fig. 19b), relationships were derived (for the area south of the APF) between chl *a* and depth and temperature and depth (e.g. Fig. 19a), based on means of all 0.5° by 1° grid cells. These relationships for January and February were then used to derive DGR versus depth using Eq. (A9). DGRs were converted to gains in wet mass as above to calculate mass increases.

Predator densities (Fig. 19c) were derived from shipboard line transects across the SW Atlantic, with data being effort-corrected (see Reid et al. 2004). Position data were converted from units of distance from land, *L* (km) to water depth, *Z* (m) using the circumpolar relationship derived from Arc GIS 9.0:

$$Z = 4727(L/136.2)^{1.76}/[1 + (L/136.2)^{1.76}],\ R^2 = 99.7\% \quad \text{(A12)}$$

We plotted representative functional groups of important land-based krill predators, penguins being represented here by Chinstrap and Macaroni penguins and flying seabirds by Antarctic Fulmar and Whitechinned petrel. Data on predator consumption (Fig. 17c) were replotted from Murphy (1995) using a similar relationship, but one specific to their study site at Bird Island, South Georgia. To show the balance-point between growth reward and predation risk (i.e. when net production is zero) we have calculated in Fig. 17d the predation probability (*p*) that exactly counteracts the increase in biomass over 9 wk:

$$B(t) = B(t+9) \quad \text{(A13)}$$

or

$$N(t)m(t) = (1-p)N(t)m(t+9) \quad \text{(A14)}$$

i.e.

$$p = 1 - m(t)/m(t+9) \quad \text{(A15)}$$

where $B(t)$, $N(t)$ denote population biomass and density, and $m(t)$ denotes mass at time t.

To provide a more specific numerical demonstration that a trade-off exists we used the estimates of annual krill consumption (tonnes wetmass km^{-2} yr^{-1}) by seabirds in relation to distance from Bird Island, South Georgia (Murphy 1995). These consumption estimates were matched against realistic values of mean krill size and density for South Georgia in January, namely 40 mm individuals (Watkins et al. 1999) with a density of 108 individuals m^{-2} (based on the mean of the 4 cells in main text Fig. 4 surrounding the island). This provides a realistic biomass of 48 g wetmass m^{-2} (Brierley et al. 1999). Growth was predicted as described above. The mortality term for a growing population was obtained by calculating the (decreasing) numbers of krill that must be removed each day to achieve the consumption values in Murphy (1995). The habitat reward is defined as net growth (i.e. gross growth – mortality), which was obtained as the product of the final predicted mass of the surviving krill and the calculated number remaining. Clearly variation in krill density (for example the approximately twofold higher krill density over shelf compared to ocean) will also affect the balance of this trade-off, with higher densities meaning proportionately lower predation risk in this model. However we have maintained density as constant in this simplest version of the model to show that predation is indeed a significant factor at South Georgia.

LITERATURE CITED

Atkinson A, Siegel V, Pakhomov EA, Rothery P (2004) Long-term decline in krill stock and increase in salps within the Southern Ocean. Nature 432:100–103

Atkinson A, Shreeve RS, Hirst AG, Rothery P and others (2006) Natural growth rates of Antarctic krill (*Euphausia superba*): II. Predictive models based on food, temperature, body length, sex, and maturity stage. Limnol Oceanogr 51:973–987

Brierley AS, Demer DA, Watkins JL, Hewitt RP (1999) Concordance of interannual fluctuations in acoustically estimated densities of Antarctic krill around South Georgia and Elephant Island: biological evidence for same-year teleconnections across the Scotia Sea. Mar Biol 134: 675–681

Godlewska M (1996) Vertical migrations of krill (*Euphausia superba* Dana). Pol Arch Hydrobiol 43:9–63

Hagen W, Kattner G, Terbrüggen A, Vleet ES (2001) Lipid metabolism of Antarctic krill *Euphausia superba* and its ecological implications. Mar Biol 139:95–104

IOC (Intergovernmental Oceanographic Commission), IHO, BODC (2003) Centenary edition of the GEBCO Digital Atlas, published on CD-ROM on behalf of the Intergovernmental Oceanographic Commission and the International Hydrographic Organization as part of the General Bathymetric Chart of the Oceans. British Oceanographic Data Centre, Liverpool

Jazdzewski K, Kittle W, Lotocki K (1982) Zooplankton studies in the southern Drake Passage and in the Bransfield Strait during austral summer (BIOMASS-FIBEX, February–March 1981). Polish Polar Res 3: 203–243

Kawaguchi S, Candy SG, King R, Naganobu M, Nicol S (2006) Modelling growth of Antarctic krill. I. Growth trends with sex, length, season and region. Mar Ecol Prog Ser 306:1–15

Mackintosh N (1973) Distribution of post-larval krill in the Antarctic. 'Discovery' Rep 36:95–156

Marr JWS (1962) The natural history and geography of the Antarctic krill (*Euphausia superba* Dana). 'Discovery' Rep 32:33–464

Miller DGM, Hampton I (1989) Biology and ecology of the Antarctic krill (*Euphausia superba* Dana): a review. BIOMASS Sci Ser 9:1–66

Moore JK, Abbott MR, Richman JG (1999) Location and dynamics of the Antarctic Polar Front from satellite sea surface temperature data. J Geophys Res C 104: 3059–3073

Murphy EJ (1995) Spatial structure of the Southern Ocean ecosystem—predator–prey linkages in Southern Ocean food webs. J Anim Ecol 64:333–347

Nicol S, Worby AP, Strutton PG, Trull TW (2004) Oceanographic influences on Antarctic ecosystems: observations and insights from East Antarctica (0° to 150° E). In: Robinson AR, Brink KH (eds) The sea. The President and Fellows of Harvard College, p 1491–1532

Orsi AH, Whitworth T, Nowlin WD (1995) On the meridional extent and fronts of the Antarctic Circumpolar Current. Deep-Sea Res I 42:641–673

Quetin LB, Ross RM (2001) Environmental variability and its impact on the reproductive cycle of Antarctic krill. Am Zool 41:74–89

Reid K, Sims M, White RW, Gillon KW (2004) Spatial distribution of predator/prey interactions in the Scotia Sea: implications for measuring predator/fisheries overlap. Deep-Sea Res II 51:1383–1396

Ross RM, Quetin LB, Baker KS, Vernet M, Smith RC (2000) Growth limitation in young *Euphausia superba* under field conditions. Limnol Oceanogr 45:31–43

Siegel V (2005) Distribution and population dynamics of *Euphausia superba*: summary of recent findings. Polar Biol 29:1–22

Tarling GA, Shreeve RS, Hirst AG, Atkinson A, Pond DW, Murphy EJ, Watkins JL (2006) Natural growth rates in Antarctic krill (*Euphausia superba*): I. Improving methodology and predicting intermolt period. Limnol Oceanogr 51:959–972

Terazaki M, Wada M (1986) Euphausiids collected from the Australian sector of the Southern Ocean during the BIOMASS SIBEX cruise (KH-83-4). Memoirs of the National Institute for Polar Research 40:97–109

Thorpe SE, Murphy EJ, Brandon MA, Stevens DP (2002) Variability of the southern Antarctic circumpolar current front north of South Georgia. J Mar Syst 37:87–105

Watkins JL, Murray AWA, Daly HI (1999) Variation in the distribution of Antarctic krill *Euphausia superba* around South Georgia. Mar Ecol Prog Ser 188:149–160

Witek Z, Kittel W, Czykieta H, Zmijewska MI, Presler E (1985) Macrozooplankton in the southern Drake Passage and Bransfield Strait in early summer 1983–1984. (BIOMASS-SIBEX). Pol Polar Res 6:95–115